Voronoi polyhedra and Delaunay simplexes in the structural analysis of molecular-dynamics-simulated materials

Witold Brostow
Departments of Materials Science and Physics, University of North Texas, Denton, Texas 76206-5310

Mieczyslaw Chybicki, Robert Laskowski, and Jaroslaw Rybicki
Department of Solid State Physics, Technical University of Gdansk, Narutowicza 11/12, 80-952 Gdansk, Poland

(Received 9 May 1997; revised manuscript received 7 October 1997)

Voronoi and Delaunay tessellations are applied to pattern recognition of atomic environments and to investigation of the nonlocal order in molecular-dynamics (MD)-simulated materials. The method is applicable also to materials generated using other computer techniques such as Monte Carlo. The pattern recognition is based on an analysis of the shapes of the Voronoi polyhedron (VP). A procedure for contraction of short edges and small faces of the polyhedron is presented. It involves contraction to vertices of all edges shorter than a certain fraction x of the average edge length, with concomitant contraction of the associated faces. Thus, effects of fluctuations are eliminated, providing ''true'' values of the geometric coordination numbers f, both local and averaged over the material. Nonlocal order analysis involves geometric relations between Delaunay simplexes. The methods proposed are used to analyze the structure of MD-simulated solid lead [J. Rybicki, W. Alda, S. Feliziani, and W. Sandowski, in *Proceedings of the Conference on Intermolecular Interactions in Matter*, edited by K. Sangwal, E. Jartych, and J. M. Olchowik (Technical University of Lublin, Lublin, 1995), p. 57; J. Rybicki, R. Laskowski, and S. Feliziani, Comput. Phys. Commun. **97**, 185 (1997)] and germianium dioxide [T. Nanba, T. Miyaji, T. Takada, A. Osaka, Y. Minura, and I. Yosui, J. Non-Cryst. Solids **177**, 131 (1994)]. For Pb the contraction results are independent of x. For the open structure of GeO_2 there is an x dependence of the contracted structure, so that using several values of x is preferable. In addition to removing effects of thermal perturbation, in open structures the procedure also cleans the resulting VP from faces contributed by the second neighbors. The analysis can be combined with that in terms of the radial distribution $g(R)$, making possible comparison of geometric coordination numbers with structural ones [W. Brostow, Chem. Phys. Lett. **49**, 285 (1977)]. [S0163-1829(98)05721-X]

I. INTRODUCTION

Contemporary computers allow the performance of molecular dynamics (MD) simulations for systems composed of hundreds of thousands of particles, which makes possible simulations of multicomponent and multiphase materials in a realistic way. The same statement applies to the materials generated on a computer by the Monte Carlo (or yet some other) procedure. Analysis of structures of perspicuous computer-simulated materials is helpful in the understanding of structure-property relationships in complex real materials, such as those including polymer liquid crystals,[1] or in polymer-based (for instance, fiber-reinforced) composites. Therefore, improving our structure analysis capabilities would be useful for all classes of materials.

One approach is based on the use of the radial distribution function $g(R)$, where R is the distance between particles (here atoms, molecules, polymer chain segments, or ions), as defined, for instance, in Ref. 2. For nonisotropic systems one also uses the angular distribution function, with both functions averaged over the whole sample volume. An analytical formula for $g(R)$ was developed already in 1976 (Ref. 3) and has been shown to provide accurate results for materials so disparate as argon, ^{4}He, neon, and sodium, including also sodium generated by Monte Carlo (MC) simulation (both MC and MD methods are described, for instance, in Refs. 1 and 2). Given $g(R)$ one can calculate the *structural* coordination number z for the kth coordination sphere around a given particle P_i:[4]

$$z_{ik}=\rho\int_{R_{\min}(k)}^{R_{\min}(k+1)} 4\pi R^2 g(R). \tag{1}$$

Here ρ is the number density equal to the number of particles per unit volume. The kth peak of $g(R)$ is located between two minima of the function $R_{\min}(k)$ and $R_{\min}(k+1)$. The index i pertains to the particle P_i and is dropped when we are dealing with z_k values for the material as a whole, such as those obtained by Fourier transforming experimental diffractometric data. The structural coordination number [maximum $z_1=12$ for the hexagonal-closed-packed (hcp) and face-centered-cubic (fcc) lattices] is usually *lower* than the average geometric coordination number f for a given material discussed below.

z_1 values are often sufficient for the characterization of regular lattices, even those containing fairly high concentrations of defects. For noncrystalline materials the knowledge of $g(R)$ diagrams plus a series of z_k values with $k\geqslant 1$ can be used. Typically for liquids and glasses one obtains fractional z_k values.[4] There are, however, at least two alternative approaches. One is the SO(3) invariants analysis[5–8] for characterization of local structures (local-order or bond-order parameters). Comparison between sets of SO(3) invariants allows for distinguishing between predefined reference patterns. The sets of invariants suitable for the identification of

the fcc, hcp, and icosahedral structures are well known,[6] but the extension of the method to other geometries is rather difficult; due to a limited number of invariants the conclusions about the local structure are not necessarily unambiguous.

The third approach—taken in the present paper—is based on the tessellation investigated in detail for sets of points by Voronoi[9,10] and subsequently applied to physical systems.[2,11–17] One uses the Voronoi polyhedron (VP) and Delaunay simplex (DS). A VP is defined as the minimal polyhedron whose planar faces bisect at right angles the lines joining a particle (these are again, atom, molecule, chain segment, or ion) to its neighbors; a pedantic definition in terms of sets is given by one of us in Ref. 15. The number of faces f_i for the ith particle is its *geometric coordination number*. Like the structural coordination numbers z_i, f_i values also can be averaged to provide f for the whole material. Values of $f=20$ or even more are known to be possible.[18] The VP diagram, also called the VP network (a set of VP's constructed for all atoms in the sample) splits in a unique manner the total sample volume into the zones owned by each particle. DS's are geometrically dual to VP's; that is, a vertex of a VP is the central site of the corresponding DS, and each particle (center of a VP) is a vertex of the corresponding DS. One can assign each vertex of the former lattice to the elementary units of the latter. The faces of DS's intersect the edges of VP's, and the faces of VP's intersect the edges of DS's. VP and DS networks contain a formidable amount of information about the structure of the sample.

The difference between VP and DS descriptions is in the access to the information. The shape of a VP reflects the arrangement of all the neighbors of the given atom. DS's represent the structure of clusters composed of four adjacent atoms. In the amorphous structures, DS's are disordered tetrahedrons, whereas VP's are more complex polyhedrons. The VP technique was applied to the analysis of the structure of the close-packed[15–17,19–24] and continuous network materials[25–27] in a relatively simple way; some statistics of the geometric properties of the polyhedrons were provided. We propose below a more systematic and direct approach to the usage of the stochastic geometry methods in the structure analysis.

The paper is organized as follows. In Sec. II we describe a procedure of the pattern recognition of atomic environments. The procedure analyzes the shapes of the Voronoi polyhedra one by one; thus it can be applied to the detection of differently structured zones in multiphase materials. In Sec. III we present a method of the nonlocal arrangement analysis based on investigation of mutual geometric relations between the elements of the Delaunay network. An application of these methods to the analysis of the MD-simulated glassy and partially crystallized lead is described Sec. IV, similar to the analysis for germanium dioxide reported in Sec. V. Section VI includes some conclusions.

II. NEIGHBOR-ARRANGEMENT RECOGNITION

The method of a local-particle arrangement spectroscopy is based on the analysis of VP shapes. VP's are constructed and analyzed recursively for all atoms in the samples, so that the individual neighborhoods are treated independently. The algorithm consists of two stages. At first, in order to eliminate the effects of small deviations from the equilibrium atom positions (due to the thermal motions), we remove from the VP network small faces and short edges. In the second stage we compare the polyhedra so constructed to certain predefined polyhedra; the number and the shapes of the latter can be arbitrary.

To demonstrate the procedure used, let us consider the influence of perturbations of atomic positions in an arbitrary crystalline lattice on their VP networks. A characteristic feature of certain crystalline (fcc, hcp, etc.) VP networks is the existence of degenerate vertices and edges. Degenerate neighbors corresponding to such vertices or edges have been defined in Ref. 15. A degenerate vertex is common to more than four edges, while a degenerate edge is common to more than three faces. As discussed also in Ref. 15, there also exist indirect neighbors: there is a common face, but the midpoint of the line connecting the atoms does not belong to that face. If the midpoint belongs to the common face, we have the simplest case of direct neighbors.[15] Here direct and indirect neighbors do not have to be distinguished; thus they are both called geometric neighbors. If the degeneracy is present, it is obvious that an arbitrary small displacement of atoms in the crystalline structure removes it. The degenerate neighbors will become the geometric ones or will cease to be the neighbors altogether. In the former case, in the place of a degenerate VP vertex a small face or a short edge will appear; degenerate edges will become small elongated faces. Thus, by eliminating short edges and small faces from the VP network by contracting them to vertices or edges, *we remove the effects of the fluctuations*. The same objective could be achieved by suitable displacements of the atoms. However, since we have no information about the individual fluctuations of the atoms in the sample, such a procedure cannot be realized in practice. In a structure in which the degenerate vertices are absent [body-centered-cubic (bcc) lattice is an example], small perturbations of the position do not change the topology of the network. Thus, the analysis of such structures can be performed going directly to the second stage of the procedure.

A. Small-face and short-edge elimination

To assure reproducibility, we need to describe in detail the procedures of elimination of small faces and short edges. The former is realized by exclusion of the geometric neighbors associated with them, followed by a repeated construction of a new VP. Figure 1 presents a distribution of face areas in a distorted hcp lattice; fcc lattice leads to similar results. Positions of points in the ideal structure are shifted by a certain distance (perturbation displacement) in a random direction. The displacements are scaled to the nearest-neighbor distance. It is seen that the faces of polyhedra can be grouped together into two sets that contain only small and only large faces. We assume that small faces are of the perturbative origin. Therefore, we need to contract all faces having an area smaller than, say, 0.2 on the average.

To contract short edges we have to use a more complicated method; there are at least two reasons for that. First, the edges can be removed only one by one, not all at the same time; this is in contradistinction to the face elimination. Second, edge lengths are very sensitive to the particle dis-

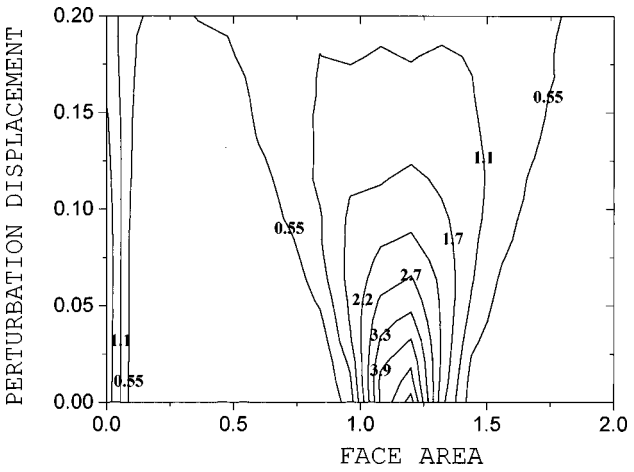

FIG. 1. The distribution function of the face areas, averaged for all VP's, plotted for a perturbed hcp lattice. The points in the structure are shifted by the perturbation displacement in a random direction. The displacements are scaled to the nearest-neighbor distance and face areas are expressed in units of the average face area.

placements. Figure 2 presents a distribution of edge lengths for a distorted hcp lattice after the face elimination. It is seen that the edges are also divided into two subsets and the short ones are of perturbative origin. The figure shows that one has to eliminate all edges shorter than about 0.5 of the average length. Because of such a high value of the rejection coefficient a special algorithm has to be applied in order to distinguish relatively long perturbative edges from the regular edges (inherent to the ideal network) of similar length so as not to eliminate too many edges. The algorithm for the short-edge contraction can be summarized as follows: (1) choose a VP, contract all edges shorter than a certain fraction x of the average edge length; (2) find the shortest edge; (3) if the edge is shorter then a fraction y $(y>x)$ of the average edge, then check the shape of the polyhedron; if the shape belongs to the set of predefined patterns, then take the next polyhedron and go to step (1); otherwise contract the edge under consideration, and go to step (2); (4) if the edge is longer then a fraction y of the average edge, then take the next polyhedron and go to step (1).

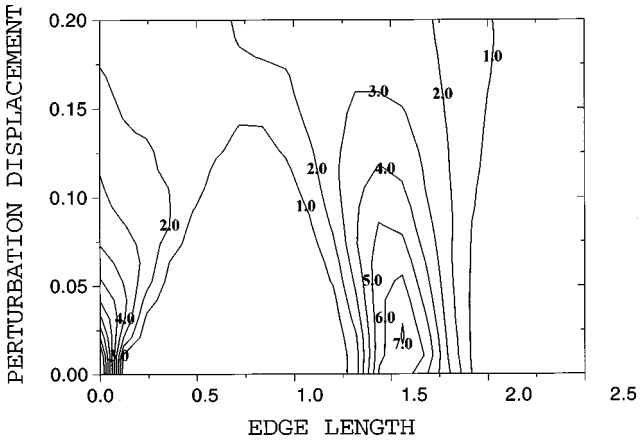

FIG. 2. The distribution of the edge lengths, averaged for all VP's plotted for a perturbed hcp lattice after the elimination of small faces. The edge length is scaled to the average edge length.

TABLE I. The F, V, and E sets for some polyhedra.

Polyhedron	F	V	E
Cube	0, 6	8, 0	12, 0
fcc	0, 12	8, 6, 0	0, 24
hcp	0, 12	8, 6, 0	3, 18, 3
Icosahedron	0, 0, 12	20, 0	30, 0
bcc	0, 6, 0, 8	24, 0	36, 0

Detailed tests of the algorithm efficiency allowed the establishment of the optimal values of the parameters x and y as 0.4 and 0.6, respectively. Taking $x<0.4$ results in switching of the shape recognition procedure sooner; if the shape of a given polyhedron is undefined, there are no consequences except for slowing down the computations. Taking $y>0.6$ for an undefined shape causes subsequent contractions, leading eventually to a polyhedron with only a few edges and a small number of faces. Once x and y are fixed at the optimal values, the elimination of small faces can be omitted in principle. These faces contain also some short edges, and the edge contraction removes them automatically. However, the initial elimination of the small faces makes the computational time considerably shorter.

B. Polyhedron shape identification

The shape of an arbitrary polyhedron can be described by three sets of integers:

$$F=(f_3,f_4,f_5,\ldots), \tag{2a}$$

$$V=(v_3,v_4,v_5,\ldots), \tag{2b}$$

$$E=(e_4,e_5,e_6,\ldots). \tag{2c}$$

f_i is the number of the i-edged faces in a polyhedron; v_i is the number of the vertices of a polyhedron from which exactly i edges originate. In the case of a nondegenerate VP, only v_3 do not vanish, hence $i-3$ determines the degeneration degree. Finally, e_i is the number of edges for which i equals $j+k+4$, where j and k are the degrees of degeneration of both vertices associated to the edge. Two polyhedrons are said to have the same topological structure if they have the same F, V, and E sets. Table I presents examples of F, V, and E sets for some polyhedrons.

We have tested the method on some perturbed crystalline lattices. As previously, the lattice points were shifted by a certain distance in a random direction. All the polyhedrons in the structures tested were correctly recognized for the displacement range lower then 0.13 of the nearest-neighbor distance. Figure 3 presents the results of the pattern recognition applied to fluctuated hcp structures. No hcp polyhedra have been detected in the structures perturbed within a displacement greater than 0.25.

III. A METHOD FOR NONLOCAL ORDER DESCRIPTION

As mentioned in the Introduction, the Delaunay network is geometrically dual to the Voronoi network. Each VP vertex can be assigned to a certain DS. Since in degenerate structures several kinds of VP vertices appear, the Delaunay

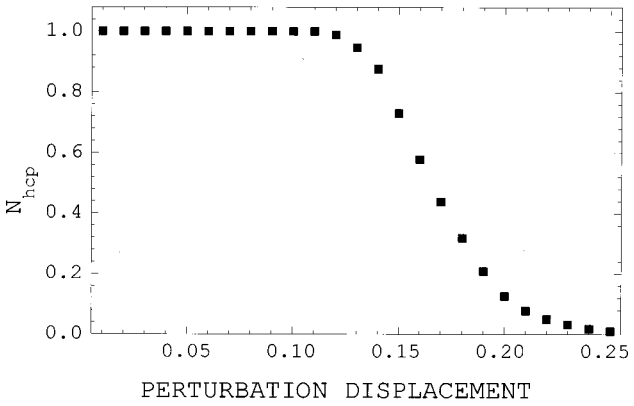

FIG. 3. The dependence of the fraction N_{hcp} of the recognized polyhedra on the perturbation displacement.

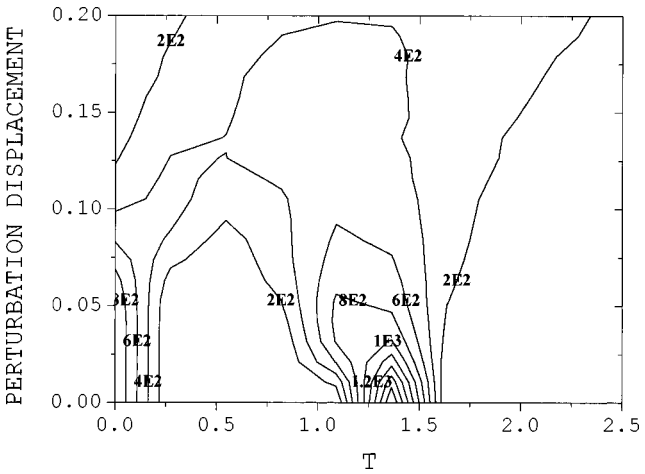

FIG. 4. The dependence of the tetrahedricity T parameter of simplexes (defined in the text) on the distortion degree of the ideal hcp lattice. All simplexes of T smaller than 0.5 are of tetrahedral origin.

network necessarily contains several types of topologically different DS's. For example, in the fcc and hcp structures one has exactly two types of VP vertices: nondegenerate ones that are associated with regular tetrahedral DS's and degenerate ones associated with octahedral DS's. One can assign more than one DS to each degenerate VP vertex. Therefore, it is helpful to introduce the definition of an *extended Delaunay simplex*, that is, a Delaunay polyhedron containing more than four atoms. Such simplexes will also be referred to as degenerate Delaunay clusters (DDC's). The geometric interpretation of DDC's is similar to that of DS's: they can be associated to vertices of the Voronoi network; however, in contradistinction to the usual Delaunay simplexes only one DDC is assigned to one degenerate vertex. Important for applications is the fact that the appearance of DDC's is a manifestation of *crystallization*. In particular, the existence of six-atom DDC's suggests that fcc or hcp regions are present in the analyzed sample. A subsequent, somewhat closer examination of the geometric relations between the DDC's reveals unequivocally the exact type of the crystalline structure.

TABLE II. The influence of the perturbation displacement ε on the parameters of the 3-, 2-, and 1-type clusters in perfect hcp sample. $N(i)$ is the number of i-element clusters, N is the number of all clusters, B is the size of the largest cluster. The hcp lattice contains 576 points.

	3-type				2-type		1-type	
ε	$N(1)$	$N(2)$	B	N	B	N	B	N
				(a) 6-atom DDC's				
0.01	0	0	6	96	576	1	576	1
0.07	0	0	6	96	576	1	576	1
0.08	0	0	6	96	566	1	566	1
0.09	2	0	6	98	554	1	554	1
0.1	6	2	6	103	534	1	534	1
0.11	15	3	6	111	498	1	498	1
0.12	21	12	15	117	461	1	461	1
0.13	34	23	17	128	425	1	425	1
0.14	42	29	14	133	389	1	389	1
0.15	42	34	12	133	360	1	360	1
				(b) Regular tetrahedral DS's				
0.01	0	576	2	576	1152	1	1152	1
0.07	0	576	2	576	1152	1	1152	1
0.08	4	572	2	576	1148	1	1148	1
0.09	27	546	2	573	1119	1	1119	1
0.1	83	483	3	567	1052	1	1052	1
0.11	128	401	5	531	937	2	938	1
0.12	181	315	4	498	806	12	818	1
0.13	215	231	4	451	662	28	693	1
0.14	232	174	4	410	544	37	594	1
0.15	239	120	4	362	195	63	490	1

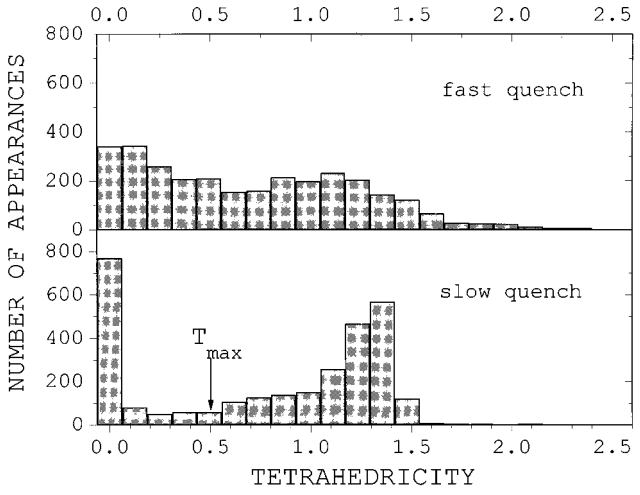

FIG. 5. The distribution of the tetrahedricity plotted for samples described in the text. T_{max} is the cutoff value for tetrahedral simplexes.

Now, using the notions introduced above, we present an efficient method for the medium- and long-range order analysis in multiphase materials. The structure recognition method is based on investigation of DS shapes, and geometric relations between DS's in structurally distinct phases. We consider the structures containing degenerate Voronoi networks. Our discussion focuses only on two examples frequently occurring in MD-simulated monatomic materials, fcc and hcp phases. Analysis of other degenerate structures can be performed in a similar way. Moreover, the investigation of any nondegenerate structure (such as bcc or random close packed) is merely a particular, and more simple case, because the DDC detection is not necessary. The method consists of two steps: elimination of lattice distortion and mutual geometric relation analysis.

A. Lattice distortion elimination

As in Sec. II, one assumes that the actual atom configuration in the system under analysis is a slightly perturbed unknown, but well-defined lattice. If the lattice is degenerate, small perturbations change the shapes of DS's, and the DDC's can be decomposed into the usual DS's. The procedure of perturbation elimination is based on the contraction of short VP network edges. The distance between the VP vertices is said to be small, if it is shorter than 0.4 of the average edge length (see again Fig. 2). This contraction is equivalent to the amalgamation of the simplexes associated to vertices that are the ends of the contracted edge. If the vertices are the ends of one edge, the corresponding simplexes have a common face (or alternatively three common atoms). Thus, amalgamating two four-atom Delaunay polyhedra we construct one five-atom DDC, amalgamating four-atom and five-atom DDC's we obtain one six-atom (octahedral) DDC, etc. To reveal the influence of the perturbation on the DS's, we use the tetrahedricity parameter T defined first by Medvedev and Naberukhin[20] and used subsequently for various purposes.[22,23] In particular, a basic difference between the liquid and amorphous solid states has been defined in terms of this parameter.[23] We have

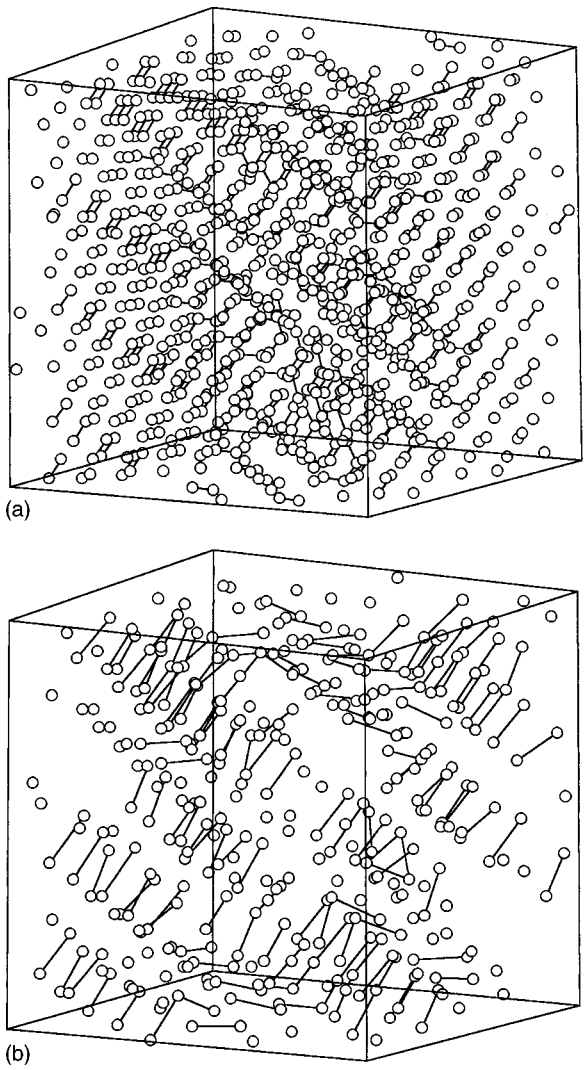

FIG. 6. The tetrahedral DS's (a) and six-atom DDC's (b) in a slowly quenched sample. The circles are centered at the centers of the simplexes (the vertices of VP's). The segments connect the neighbors in terms of the 3 relation.

$$T=\sum_{i,j}(l_i-l_j)^2/l^2, \tag{3}$$

where l_i is the length of the ith Delaunay simplex edge; l is the average edge length of the simplex. As an example, we show the dependence of the T parameter on the perturbation in the hcp lattice in Fig. 4. An analogous plot for the fcc lattice is identical. It turns out that all DS's for T smaller than 0.5 *originate from regular tetrahedra.*

B. Geometric relations between Delaunay polyhedrons

At this stage we analyze geometric relations between DS's and between DDC's inherent to certain reference patterns, and those detected in the MD-simulated sample under consideration. In the case of fcc and hcp lattices we have, respectively, regular tetrahedral DS's and octahedral DDC's. In the former, the vertices of the VP network assigned to DS's are never the ends of an edge. A similar situation is found in the case of DDC's. Thus, each edge ends with vertices belonging to different types of the Delaunay clusters

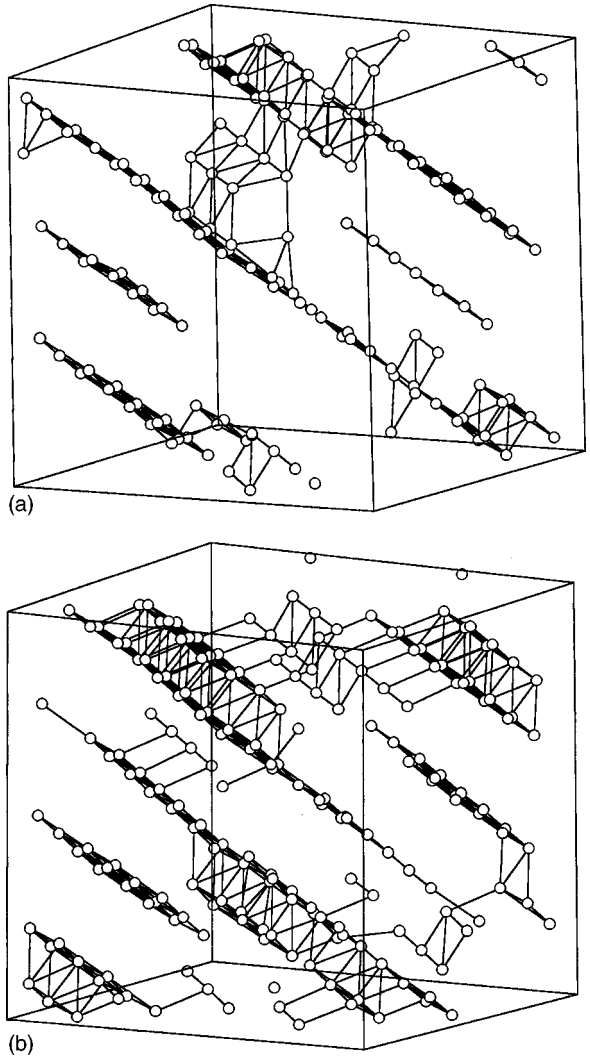

FIG. 7. The (a) fcc- and (b) hcp-coordinated atoms in a slowly cooled sample. The circles are centered at the Pb atoms that have fcc (a) or hcp (b) neighborhoods. The lines connect geometric neighbors.

(DS's and DDC's are both Delaunay clusters). The regular tetrahedral DS is connected by two atoms (an edge) to another DS, and a similar statement applies to DDC's. Thus, tetrahedral simplexes and octahedral DDC's compose infinite three-dimensional clusters. In the hcp structure, the tetrahedral simplexes share a common face, producing two-element clusters. The double clusters naturally have one common edge. The octahedral DDC's are connected by the faces and compose infinite linear clusters, parallel to the axes of double tetrahedral clusters.

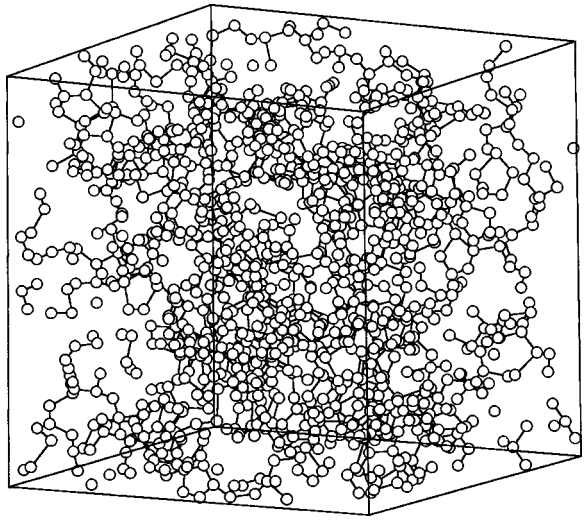

FIG. 8. The tetrahedral simplexes in a quickly quenched sample. Circles and edges as in Fig. 6.

Let us introduce a notation that will be helpful in the description of geometric relations in the sets of DS's and DDC's. When two simplexes share three atoms, we say that they remain in a ''3-relation''; if they share at least two atoms, there is a ''2-relation.'' Finally, if the Delaunay polyhedra share at least one atom, we say that they are in a ''1-relation.'' The 3-relation implies the 1- and the 2-relations, and the 2-relation implies the 1-relation, but not the 3-relation.

Given this terminology, we see that we can construct 3-type, 2-type, and 1-type clusters of DS's or DDC's. A DS (DDC) belongs to an i-type cluster if it is i related to any element of this cluster. So a 1-type cluster contains 2- and 3-type clusters, etc. Mutual geometric relations between DS's (or DDC's) in any sample under analysis can be described in a very concise form. In the case of the fcc structure, tetrahedral simplexes and octahedra are isolated in respect to the 3-relation, whereas in respect to the 2- and 1-relations they compose infinite clusters, containing all atoms of the sample. In the hcp phase, tetrahedral simplexes are arranged in double 3-type clusters, and infinite 2- and 1-type clusters, whereas octahedra form an infinite linear 3-type cluster.

TABLE III. The results of the Delaunay network analysis performed for slowly and quickly quenched Pb. The columns are described in the caption of Table II.

	3-type			2-type		1-type		
	$N(1)$	$N(2)$	B	N	B	N	B	N
	(a) Clusters of 6-atom DDC's							
Fast	50	17	9	89	168	2	169	1
Slow	60	79	7	197	422	1	422	1
	(b) Clusters of the tetrahedral simplexes							
Fast	45	3	998	62	1135	1	1135	1
Slow	363	210	24	619	958	1	958	1

TABLE IV. Number of faces in Voronoi polyhedra of Ge atoms. The faces can be associated to neighboring oxygen or germanium. The polyhedra are not contracted.

Number of polyhedra (%)	Ge	O
17.8	0	7
15.6	0	8
11.4	0	6
9.4	0	9
6.6	1	8
6.0	1	9
4.8	1	7
4.4	1	10
4.4	0	10
2.8	1	6
2.6	0	5
2.6	1	11
2.2	0	11
2.0	1	12
1.6	2	10
1.2	2	8

The comparison of the shapes and sizes of the 3-, 2- and 1-type clusters in the sample with the clusters determined for the predefined reference structures allows one to draw some conclusions concerning the nonlocal arrangement. For example, if in any region of the sample one finds about two times more tetrahedral simplexes than octahedral DDC's, and they are rather isolated as far as 3-relations are concerned, we infer that the region has the fcc structure. If there is a large 3-type cluster of tetrahedral simplexes in the sample, we are dealing with a random-close-packed (rcp) glass. Table II presents the influence of perturbations of the ideal hcp structures on properties of 3-, 2-, and 1-type clusters. It is seen that for fluctuations greater than 8%, the clusters of tetrahedral DS's and octahedral DDC's become different from the ones expected in an unperturbed structure.

A similar analysis can be performed for other kinds of phases. For example, the bcc phase has only DS's of T equal to 0.203; thus they compose one infinite three-dimensional cluster in terms of the 3-relation. Detection of bcc simplexes consists in the rejection of simplexes that have very low as well as very high values of the tetrahedricity parameter defined by Eq. (3).

IV. ANALYSIS OF MD-SIMULATED SOLID Ph

As an example, we apply our method to the analysis of the local arrangement and the nonlocal ordering in two samples of MD-simulated lead.[28,29] The simulations have been performed in the microcanonical ensemble using an experimental pair-interaction potential of Dzugutov, Larsson, and Ebbsjo[30] obtained by a careful fitting of the MD results to the static structure factor $S(k)$ at 623 K (23 K above the melting temperature). The interaction potential $u(r)$ contains hard-core and soft-core repulsion terms, and also an oscillatory long-range Friedel component:

$$u(r)=u_1(r)+u_2(r)+u_3(r),$$

$$u_1(r)=a_1(b_1/r)^{12}\exp[(r-c_1)^{-1}], \quad r<c_1,$$

$$u_1(r)=0, \quad r\geqslant c_1,$$

$$u_2(r)=a_2(b_2/r-c_2)\exp[(r-b_2)^{-1}], \quad r<b_2,$$

$$u_2(r)=0, \quad r\geqslant b_2,$$

$$u_3(r)=a_3 r^{-3}\cos(2K_F r). \tag{4}$$

The following values of the parameters were used: $a_1=102.5$ meV, $b_1=0.3284$ nm, $c_1=0.572$ nm, $a_2=90$ meV, $b_2=0.483$ nm, $c_2=0.5$, $a_3=0.4183$ meV nm^3, and $K_F=15.417$ nm^{-1}. The samples were prepared initially as well-equilibrated hot liquids of various densities (or alternatively under various pressures), and quenched at constant volume, and at various cooling rates down to 1 K. The results reported below pertain to samples with high density equal to 150×10^2 kg/m^3. We recall that the experimental value of the density of Pb at the melting point is 106.9×10^2 kg/m^3. The samples were either quenched to 1 K directly from 5000 K (fast cooling), or else passed through equilibrium states at 2500 K, 1250 K, 600 K, 300 K, and 150 K (slow cooling). Each sample contained 500 Pb atoms.

The distribution of the tetrahedricity of the DS's is shown in Fig. 5. It is seen that the slowly cooled sample contains only regular tetrahedral ($T\approx0$) and octahedral ($T>1$) simplexes, which suggests the existence of fcc or hcp zones. The cutoff value for tetrahedral simplexes is equal to 0.5. Parameters of the 3-, 2-, and 1-type clusters are presented in Table III. The large number of the tetrahedral simplexes that are isolated or appear in double clusters confirms the existence of fcc and hcp phases. The tetrahedra isolated in terms of the 3-relation are characteristic for the fcc structure, whereas the double clusters for the hcp configuration. Figure 6 presents the arrangement of the regular tetrahedral DS's and six-atom DDC's in the simulation box. A laminar arrangement of DS's and DDC's is evident. The fcc and hcp neighborhoods that have been found are shown in Fig. 7 (the parameters x, y of the edge contraction were equal to 0.4 and 0.6, respectively, and all the faces with areas smaller than 0.2 of the average value have been contracted). 154 atoms of fcc-like first neighborhood, and 199 atoms of hcp-like neighborhood were detected. The laminar arrangement of the fcc and hcp phases is clearly seen. We infer that the bcc or other environments, if present, would be detected as well.

The quickly cooled sample has a quite different structure. The tetrahedricities of the DS's change in a wide range (from 0 to more than 1.5, Fig. 3), but small peaks at about $T=0$ and 1.3 are still present. The large number of tetrahedral simplexes (Table III) and a large size of the 3-type clusters suggest that the sample has a glassy structure (rcp). Figure 8 shows the arrangement of the tetrahedral simplexes. No atoms with the fcc or hcp local arrangement have been detected, and only two atoms have a full icosahedral neighborhood.

V. APPLICATION OF THE CONTRACTION TECHNIQUE TO OPEN STRUCTURES

The example of lead, while quite instructive, does not tell us how the new procedure would work for open structures.

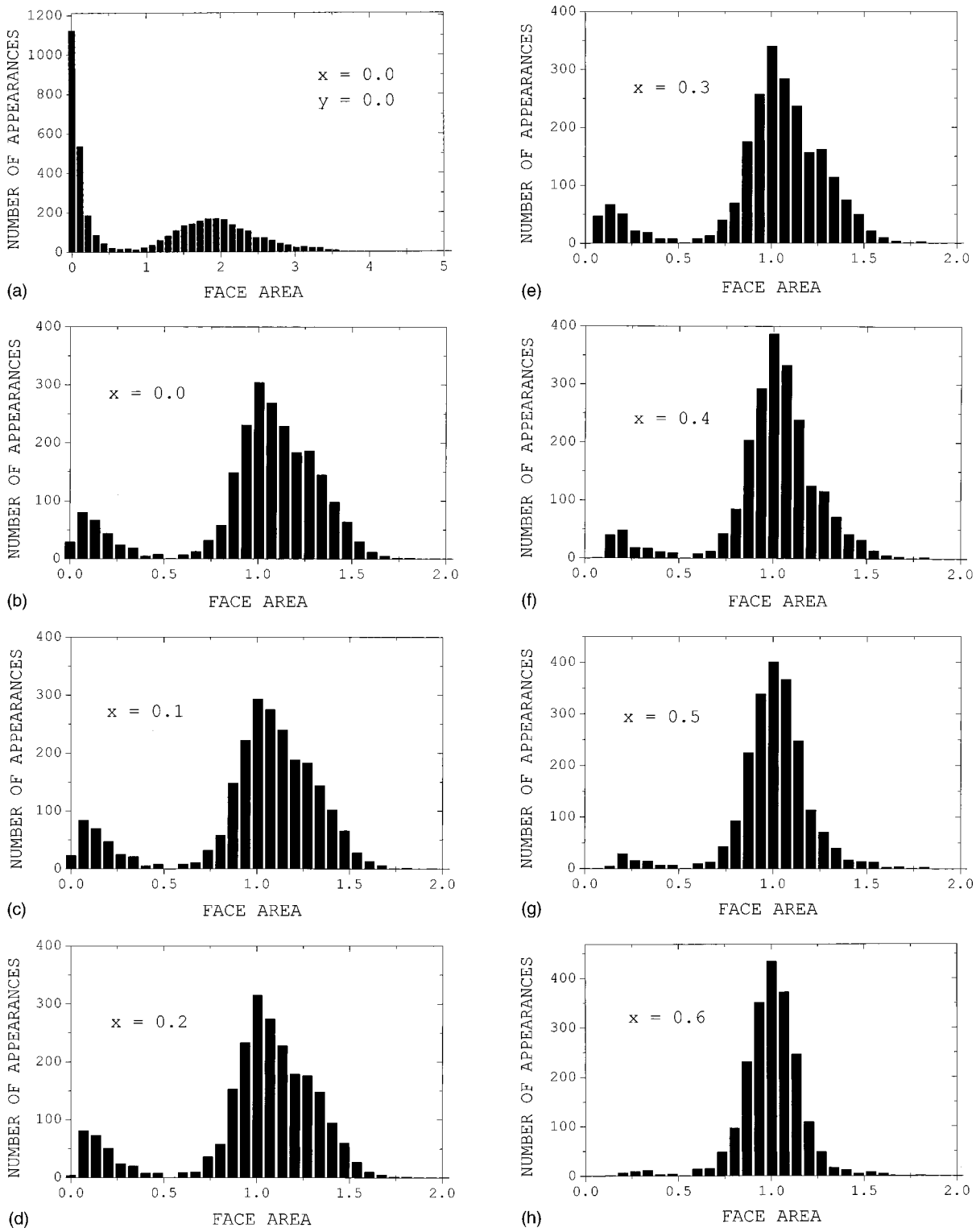

FIG. 9. Statistics of polyhedra face areas for various values of x; $y=0.6$, except in (a). Face areas are expressed in units of the average face area of a given polyhedron.

Therefore, we have applied the contraction method also to the analysis of germanium dioxide, namely, to local neighborhoods of Ge atoms in a MD-simulated GeO_2 sample. Our simulation box contained 500 Ge atoms and 1000 O atoms interacting via the Born-Mayer pair potential, with the parameters defined by Nanba *et al.*[31] The simulation was performed in the constant pressure ensemble with a random initial configuration. The sample was thermalized for 4×10^4 simulation femtosecond time steps at 300 K.

We have constructed the Voronoi polyhedra for Ge atoms as the central ones. As seen in Table IV, Ge-atom polyhedra share faces mainly with oxygen polyhedra, but there is a significant number of polyhedra with faces (always very small) associated to Ge. Distribution of the face areas presented in Fig. 9(a) shows that noncontracted polyhedra consist of a nearly equal number of big and much smaller faces

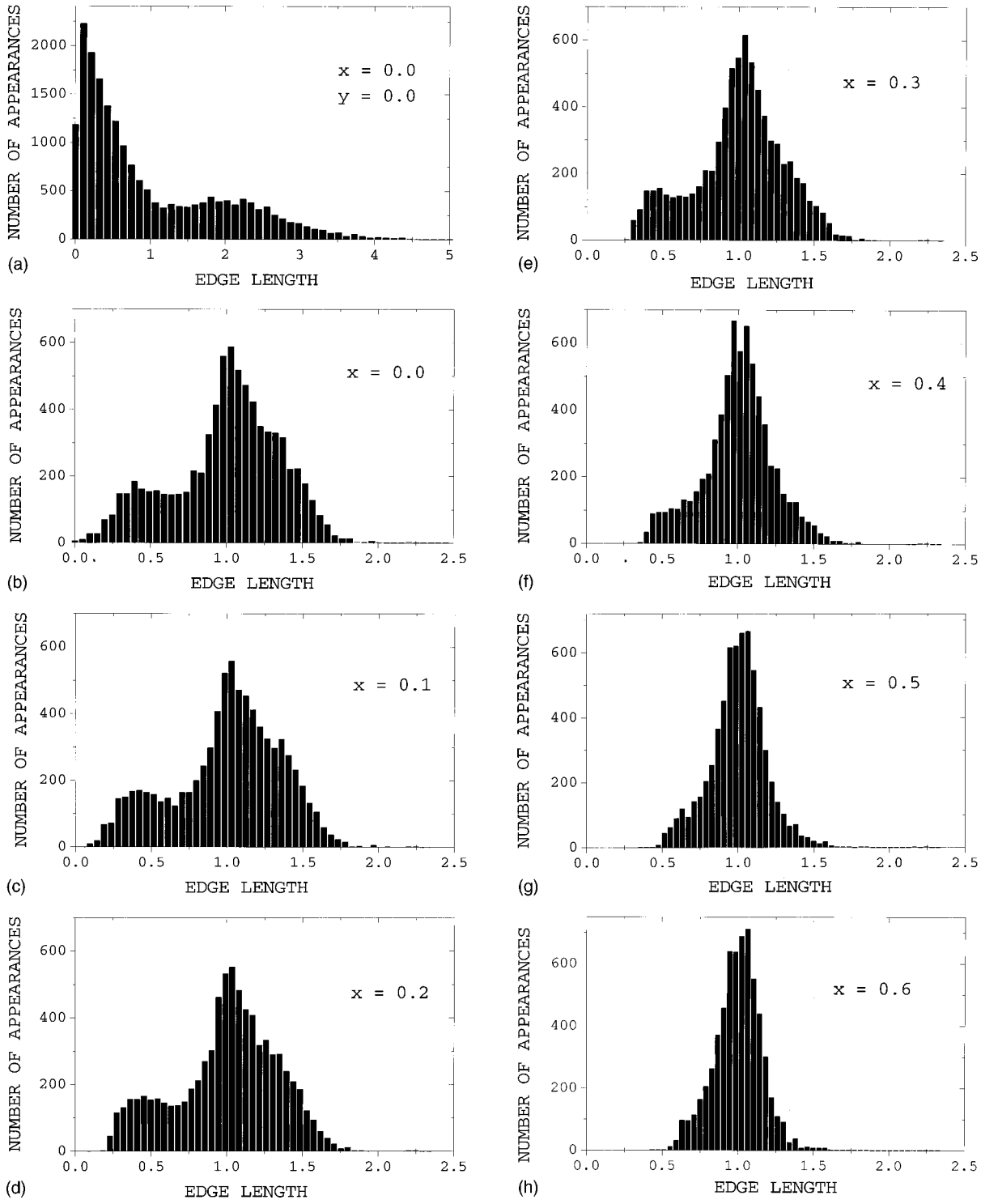

FIG. 10. Statistics of polyhedra edge lengths for various values of x; $y=0.6$, except in (a). Edge lengths are expressed in units of the average edge length of a given polyhedron.

(average number of faces per polyhedron equals 8.1). We can see two well-separated peaks. This suggests that mainly *trigonal pyramids with oxygen atoms in vertices* constitute the local Ge neighborhoods; the smaller faces originate from further neighbors. In the case of distribution of edge lengths presented in Fig. 10(a), due to quadratic dependence of face areas on edge lengths, these peaks are not so well separated but still remain visible. In order to show how the contraction procedure deals with an open structure of GeO_2, we performed several contractions for $0.0 \leqslant x \leqslant 0.6$, and $y=0.6$. In Tables V and VI one can see that the number of faces of polyhedra and their shapes are almost x independent in the interval $0.0 \mapsto 0.2$. There we have mainly two kinds of local neighborhoods: trigonal pyramids and trigonal bipyramids. As x increases beyond 0.2, the number of the latter decreases while the number of the former increases. A similar behavior appears in the case of square pyramids and square bipyramids; their overall number is much smaller, however. Such a

TABLE V. Number of faces in contracted polyhedra of Ge atoms. All faces are associated to oxygen, $y=0.6$.

	Number of Ge atoms (%)	O
$x=0.0$	52.0	5
	44.6	4
	1.8	6
$x=0.1$	54.2	5
	42.6	4
	1.8	6
$x=0.2$	52.8	5
	44.8	4
$x=0.3$	1.6	6
	45.6	5
	53.2	4
$x=0.4$	68.8	4
	30.2	5
$x=0.5$	81.4	4
	17.8	5
$x=0.6$	90.4	4
	8.8	5

dependence follows from the fact that Voronoi polyhedra of atoms with neighborhood types such as the trigonal bipyramid and the square bipyramid contain one small triangular face; with increased x this face disappears during contraction. Distributions of face areas and edge lengths are presented in Figs. 9 and 10. It is seen that the peak of small edges is visible well up to $x=0.3$. For faces this peak does not disappear.

We find that the results of our contraction procedure may depend on x for open structures. This is so because a low geometric coordination number f implies a relative simplicity of the Voronoi polyhedra topology. During the contraction process a polyhedron is modified, and after each edge contraction we obtain a new shape. If the length of a contracted edge is larger than x, and the polyhedron shape belongs to a predefined set, the procedure terminates not necessarily arriving at the optimal shape. With a certain practice, parameters x and y are chosen so as to assure the maximum efficiency of the method. This relies on experience and does not sound precise, but there are at least two procedures that can be used. First, one can perform several contractions for various values of x, thus generating more information about the structures. Second, one can assume, for instance, $x=0.1$ for open and $x=0.4$ for closed structures and then compare results for different systems for fixed x. For all structures $y=0.6$ can be taken.

The information so obtained can be combined with the knowledge of the radial distribution function $g(R)$ discussed briefly in Sec. I. For open structures the structural coordination number z calculated from Eq. (1) can then be compared with the geometric coordination number f for a fixed x, or with several $f(x)$ values obtained from a series of contractions. In contradistinction to open structures, for close-packed structures there is no dependence of the contraction results on x.

TABLE VI. Dependence of the shapes of the Voronoi polyhedra on x, $y=0.6$.

$x=0.0$	Trigonal pyramid	44.6%
	Trigonal bipyramid	51.2%
	Square bipyramid	1.6%
	Square pyramid	1.0%
$x=0.1$	Trigonal pyramid	42.6%
	Trigonal bipyramid	53.2%
	Square bipyramid	1.6%
	Square pyramid	1.4%
$x=0.2$	Trigonal pyramid	44.8%
	Trigonal bipyramid	51.0%
	Square bipyramid	1.4%
	Square pyramid	2.0%
$x=0.3$	Trigonal pyramid	53.2%
	Trigonal bipyramid	42.8%
	Square pyramid	2.8%
$x=0.4$	Trigonal pyramid	68.8%
	Trigonal bipyramid	26.6%
	Square pyramid	3.6%
$x=0.5$	Trigonal pyramid	81.4%
	Trigonal bipyramid	14.2%
	Square pyramid	3.6%
$x=0.6$	Trigonal pyramid	90.4%
	Trigonal bipyramid	5.4%
	Square pyramid	3.4%

VI. CONCLUDING REMARKS

Space tesselations have been studied by the Ukrainian mathematician Voronoi approximately a century ago;[9,10] with time, his work finds more and more uses.[32–34] We have demonstrated the applications of the Voronoi and Delaunay tessellations to the analysis of local and nonlocal arrangements in MD-simulated materials. The Voronoi polyhedra allow definition of the neighborhoods of atoms in disordered samples in a simple way, and the classification of the neighbors, including direct and degenerate ones. The contraction of faces and edges of the polyhedra has a clear geometric significance: it simply changes the category of a neighbor. Therefore, the procedure of the local-order recognition can be interpreted as a virtual rearrangement of geometric neighbors present in the initial disordered structure. As shown in Sec. II, the procedure is efficient for lattices disordered with the perturbation displacement up to 13% of the nearest-neighbor distance. For fluctuations lower then 15% no polyhedra other than the original ones have been detected for the Pb system; this proves that for closed structures the method leads to unambiguous results. For perturbations greater than 25% no polyhedra were recognized in the Pb material. Thus, the method has a relatively low efficiency for simulated materials with wide minima of the potentials. The results for solid Pb show that in closed systems our procedure can be successfully applied to the detection of any phase present within the MD simulation box. The Delaunay simplexes can be applied to investigate the nonlocal order. In particular, the analysis of the properties of the 3-, 2-, and 1-type clusters defined in this work allows the description of the nonlocal ordering, and also enables direct comparisons of structures of

different amorphous samples. In contradistinction to the VP approach, the cluster method works also for extremely small (embryolike) crystalline zones in which the atoms do *not* have a well-defined crystalline neighborhood.

ACKNOWLEDGMENTS

Partial support for this work was provided by the North Atlantic Treaty Organization, Brussels (Award No. HTECH.LG 960084) and by the State of Texas Advanced Technology Program, Austin (Award No. 003661-047). We appreciate discussions with Professor József Karger-Kocsis, University of Kaiserslautern, and with Professor Michael Bratychak and his colleagues at the Lvivska Politechnika State University. We acknowledge the Trójmiejska Akademicka Siec Komputerowa (TASK) Computer Center, Gdansk, for the opportunity to perform our numerical calculations.

[1] W. Brostow, in *Polymer Liquid Crystals: Mechanical and Thermophysical Properties*, edited by W. Brostow (Chapman & Hall, London, 1998), Chap. 15.
[2] W. Brostow, *Science of Materials* (Wiley, New York, 1979); *Science of Materials* (Krieger, Malabar, 1985); *Introducción a la Ciencia de los Materiales* (Editorial Limusa, México City, 1981); *Einstieg in die Moderne Werkstoffwissenschaft* (VEB Deutscher Verlag für Grundstoffindustrie, Leipzig, 1985); *Einstieg in die Moderne Werkstoffwissenschaft* (Carl Hanser Verlag, München-Wien, 1985).
[3] W. Brostow and J. S. Sochanski, Phys. Rev. A **13**, 882 (1976).
[4] W. Brostow, Chem. Phys. Lett. **49**, 285 (1977).
[5] P. Steinhard, D. Nelson, and M. Ronchetti, Phys. Rev. B **28**, 784 (1983).
[6] S. Ogata and S. Ichimaru, Phys. Rev. A **39**, 1333 (1989).
[7] A. Mitus and A. Patashinskii, Physica A **150**, 371 (1988); A. Mitus, D. Marx, S. Sengupta, P. Nielaba, A. Patashinskii, and H. Hahn, J. Phys.: Condens. Matter **5**, 8509 (1993).
[8] H. Gades and A. Mitus, Physica A **176**, 297 (1991).
[9] G. Voronoi, J. Reine Angew. Math. **134**, 198 (1908).
[10] G. Voronoi, J. Reine Angew. Math. **136**, 67 (1909).
[11] R. Collins, Proc. Phys. Soc. London **86**, 199 (1965).
[12] J. L. Finney, Proc. R. Soc. London, Ser. A **319**, 479 (1970); **319**, 495 (1970).
[13] W. Brostow and Y. Sicotte, J. Stat. Phys. **9**, 339 (1973).
[14] W. Brostow and Y. Sicotte, Physica A **80**, 513 (1975).
[15] W. Brostow, J.-P. Dussault, and B. L. Fox, J. Comput. Phys. **29**, 81 (1978).
[16] M. Tanemura, T. Ogawa, and N. Ogita, J. Comput. Phys. **51**, 191 (1983).
[17] N. N. Medvedev, J. Comput. Phys. **67**, 223 (1986).
[18] F. W. Smith, Can. J. Phys. **43**, 2052 (1965).
[19] Y. Hiwatari and T. Saito, J. Chem. Phys. **81**, 6044 (1984).
[20] N. N. Medvedev and Y. I. Naberukhin, J. Non-Cryst. Solids **94**, 402 (1987).
[21] V. Krishanamurthy, W. Brostow, and J. S. Sochanski, Mater. Chem. Phys. **20**, 451 (1988).
[22] N. N. Medvedev, V. P. Voloshin, and Y. I. Naberukhin, J. Phys. A **21**, L247 (1988).
[23] N. N. Medvedev, A. Geiger, and W. Brostow, J. Chem. Phys. **93**, 8337 (1990).
[24] V. A. Likhachev, A. I. Mikhailin, and L. V. Zhigilei, Philos. Mag. A **69**, 421 (1994).
[25] J. R. Rustand, A. D. Yuen, and F. J. Spera, Phys. Rev. B **44**, 2108 (1991).
[26] K. Tsumuraya, K. Ishibasihi, and K. Kusunoki, Phys. Rev. B **47**, 8552 (1993).
[27] M. Liska, P. Perichta, and B. Hatalova, Phys. Chem. Glasses **36**, 63 (1995).
[28] J. Rybicki, W. Alda, S. Feliziani, and W. Sadowski, in *Proceedings of the Conference on Intermolecular Interactions in Matter*, edited by K. Sangwal, E. Jartych, and J. M. Olchowik (Technical University of Lublin, Lublin, 1995), p. 57.
[29] J. Rybicki, R. Laskowski, and S. Feliziani, Comput. Phys. Commun. **97**, 185 (1997).
[30] M. Dzugutov, K. E. Larsson, and I. Ebbsjo, Phys. Rev. A **38**, 3609 (1988).
[31] T. Nanba, T. Miyaji, T. Takada, A. Osaka, Y. Minura, and I. Yosui, J. Non-Cryst. Solids **177**, 131 (1994).
[32] V. P. Privalko and V. V. Novikov, *The Science of Heterogenous Polymers* (Wiley, Chichester/New York, 1995), Sec. 4.2.
[33] Voronoi Memorial Volume prepared by the Institute of Mathematics of the National Academy of Sciences of Ukraine, Kyiv (unpublished).
[34] W. Brostow, J. Mater. Educ. (to be published).